

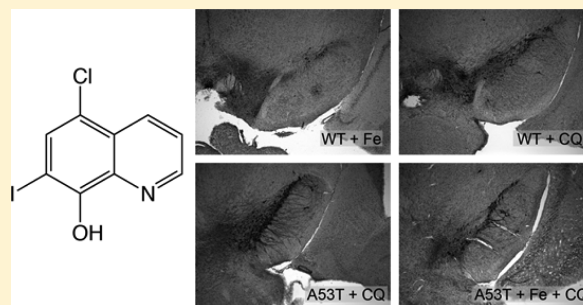
Effects of Neonatal Iron Feeding and Chronic Clioquinol Administration on the Parkinsonian Human A53T Transgenic Mouse

Jessica L. Billings,^{†,§} Dominic J. Hare,^{†,‡,§} Milawaty Nurjono,[†] Irene Volitakis,[†] Robert A. Cherny,[†] Ashley I. Bush,[†] Paul A. Adlard,[†] and David I. Finkelstein^{*,†}[†]The Florey Institute of Neuroscience and Mental Health, The University of Melbourne, Parkville, Victoria 3052, Australia[‡]Elemental Bio-imaging Facility, University of Technology Sydney, Broadway, New South Wales 2007, Australia

Supporting Information

ABSTRACT: Increased nigral iron (Fe) is a cardinal feature of Parkinson's disease, as is the accumulation of aggregates comprising α -synuclein. We used wild-type mice and transgenic mice overexpressing the human A53T mutation to α -synuclein to examine the influence of increased Fe (days 10–17 postpartum) on the parkinsonian development phenotype of these animals (including abnormal nigral Fe levels and deficits in both cell numbers and locomotor activity), and to explore the impact of the Fe chelator clioquinol in the model. Both untreated and Fe-loaded A53T mice showed similar levels of nigral cell loss, though 5 months of clioquinol treatment was only able to prevent the loss in the non-Fe-loaded A53T group. Iron levels in the Fe-loaded A53T mice returned to normal at 8 months, though effects of dopamine denervation remained, demonstrated by limited locomotor activity and sustained neuron loss. These data suggest that Fe exposure during a critical developmental window, combined with the overexpression mutant α -synuclein, presents a disease phenotype resistant to intervention using clioquinol later in life.

KEYWORDS: Parkinson's disease, α -synuclein, iron accumulation, dietary iron, risk factor



Iron (Fe) is an essential bioelement that plays numerous roles in the healthy brain.¹ However, several chronic neurodegenerative diseases, particularly Parkinson's disease (PD), have shown marked deposition of Fe in vulnerable brain regions² beyond that typical of normal accumulation with age.³

The human A53T mutation to the α -synuclein (SNCA) gene has been widely associated with familial early onset PD, as these mutant peptides demonstrate an increased capacity to self-assemble and form what are thought to be toxic Lewy body inclusions within the substantia nigra pars compacta (SNc) region of the brain.⁴ In cell culture, aggregation of mutant A53T α -synuclein (hereafter, α -syn) is potentiated by iron and demonstrates increased neurotoxicity.⁵ Increased iron alone in the mouse SNc has been associated with increased dopaminergic neurodegeneration in mice;⁶ thus, it stands to reason that a combined model encompassing both elevated iron and the A53T mutation presents a more comprehensive model to study the effects of these two pathological features of PD.

We recently demonstrated that clioquinol (iodochlorhydroxyquin-8-ol; CQ; Figure 1A), a first generation 8-hydroxyquinoline, partially rescued the parkinsonian phenotype present in the A53T mutant mouse model.⁷ Clioquinol has a moderate affinity for Fe,⁸ and has been demonstrated as an effective means for reducing toxicity following 1-methyl-4-phenyl-1,2,3,6-tetrahydropyridine (MPTP) insult,⁹ which is known to elevate nigral Fe levels.¹⁰

In this study, we expanded our investigations to examine the effects of supplementary loading of the postnatal mouse brain with Fe to potentiate A53T-Fe neurotoxicity, and then investigate the possible use of CQ as a means to reduce cell damage and improve motor function. Early life Fe exposure has been proposed as a possible risk factor for PD,¹¹ and has been shown to stimulate midbrain neurodegeneration with age,¹² neurobehavioral dysfunction¹³ and enhance MPTP toxicity in wild type mice.^{12,14} Elevation of brain Fe appears to be a feature of both sporadic and familial forms of PD, with increased nigral Fe observed in PD cases featuring mutations to the SNCA, PARK2, PINK1, PARK7, and PARK8 genes.¹⁵

Therefore, it is important to examine the effects of potential Fe-targeting drugs in disease models that recapitulate not only brain Fe accumulation, but also genetic features found in familial forms of PD. Here, we used normal mice and a mouse model overexpressing the human A53T point mutation to SNCA, the gene encoding α -syn,¹⁶ and introduced an additional parkinsonian paradigm—neonatal Fe overload,¹² to further assess the potential of CQ as a modulator of this PD-like pathology.

Received: November 23, 2015

Accepted: December 28, 2015

Published: December 29, 2015



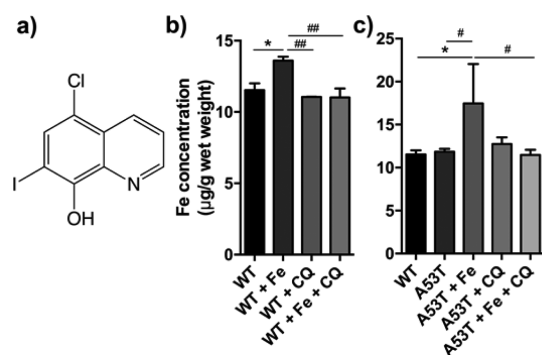


Figure 1. (a) Structure of iodochlorhydroxyquin-8-ol (clioquinol; CQ). (b) Analysis of SNc tissue digests by ICP-MS demonstrated that neonatal Fe supplementation significantly increased nigral Fe in the SNc, which was ameliorated by subsequent treatment with CQ for 5 months. (c) The A53T-Fe fed group also demonstrated increased nigral Fe content compared to both wild type and non-Fe fed A53T animals. Control Fe levels were similarly restored by CQ administration (* or # $p < 0.05$; one-way ANOVA with Fisher's LSD test; *compared to WT control; #compared WT or A53T Fe supplementation).

RESULTS AND DISCUSSION

Eight experimental groups of animals (see [Methods](#)) were exposed to either an 8% sucrose vehicle or vehicle supplemented with 0.12 mg kg⁻¹ body weight of Fe 10–17 days postpartum. Wild-type (WT; C57BL/6 as a genetic background) controls and A53T transgenic fed either vehicle or a regime of supplemented Fe were allowed to age normally. One group of vehicle-treated WT and A53T mice were fed an average of 37 mg kg⁻¹ body weight of CQ as part of their normal dietary intake, while the remaining Fe-supplemented groups were also administered an equivalent dose of CQ. Clioquinol administration commenced at 12 weeks of age and continued for 5 months in total. Our experimental design was intended to examine the use of CQ as a preclinical therapy for addressing brain Fe overload, as the treatment protocol was thus envisioned as an interventionist approach, as the A53T transgenic mouse does not exhibit evidence of cellular synucleinopathy until 6 months of age or a motor phenotype until 7–8 months.¹⁶

Neonatal iron intake significantly increased Fe levels in the SNc of both Fe-fed WT and A53T mice compared to untreated WT (WT + Fe = +18.0%, $p < 0.05$; A53T + Fe = +51.4%, $p < 0.05$; one-way ANOVA with Fisher's least significant difference [LSD] test; [Figure 1B, C](#)), as measured by inductively coupled plasma-mass spectrometry (ICP-MS) of tissue collected after animals were culled at 8 months of age. The WT and A53T groups exposed to high neonatal iron and subsequent CQ treatment demonstrated a return to normal levels of Fe (−3.0%, $p = 0.90$), as did CQ-treated WT (−4.4%, $p = 0.55$). To determine if neonatal Fe feeding resulted in region-specific Fe accumulation, and if CQ treatment resulted in a decrease in non-nigral tissue, we also measured total Fe concentration in caudate putamen, cortex, and cerebellum ([Supporting Information Table S1](#)) and found no difference between treatment groups in these brain regions, except for a decrease in the caudate putamen in CQ-only treated WT mice (−26.4%; $p < 0.01$). In the healthy mouse brain, these regions typically contain markedly lower Fe concentrations than midbrain structures, including the SNc.¹⁷

To examine the effects of chronic CQ administration on neuronal survival in the SNc, we stained sections for tyrosine hydroxylase (TH; the rate-limiting enzyme in dopamine synthesis¹⁸) and counterstained with neutral red ([Figure 2A](#)). As stated previously, the A53T transgenic first demonstrate synucleinopathy or disease phenotype at 6–8 months, and it was originally reported that diffuse synuclein pathology was confined to the cerebellum, cortex and motor neurons of the spinal cord,¹⁶ though this study did not examine SNc cell numbers. In line with our previous report,⁷ damage appears to also manifest in the basal ganglia. There was a significant decline in SNc neuron numbers in the untreated A53T transgene alone compared to background control (−19.3%; $p < 0.001$; [Figure 2B](#)), confirming our previous reports.^{19,20} Stereological cell counts also revealed a significant decline in neuron numbers in the Fe-supplemented A53T animals (−17.4%; $p < 0.01$), though it is not apparent that the supplementary Fe contributed to increased cell death. However, while CQ administration to A53T only mice elicited the predicted recovery in neuron numbers (−3.92%; $p = 0.3$), confirming our previous report,⁷ CQ was unable to produce the same effect in Fe-supplemented A53T animals (−25.4%; $p < 0.001$). The observed effect was confined to dopaminergic neurons, with non TH-positive neurons not significantly changed in any experimental group ([Figure 2C](#)). This finding is intriguing, as we have previously shown that CQ inhibit the formation of potentially insoluble toxic α -syn fibrils,⁷ as well as aggregation of the toxic β -amyloid protein implicated in Alzheimer's disease;²¹ with the latter study suggesting this mechanism is independent of the presence of metal ions.

As Fe is associated with oxidative stress in PD, we examined the levels of protein carbonyls in a small subset from both experimental groups ($n = 5$). For the WT animals, neonatal Fe loading significantly increased the amount of oxidative damage (+51.9%, $p < 0.05$), and CQ treatment returned carbonyl levels to control ([Figure 3](#)). Unexpectedly, protein carbonyl levels were lower across the board in the A53T group compared to WT, and comparisons of CQ-treated, Fe-loaded A53T mice revealed no significant differences. We note that these results should be interpreted with caution due to the small sample size used and large intragroup variance observed.

Our findings suggest that early life Fe exposure may present a chemical environment within dopaminergic neurons during neurodevelopment that is irrecoverable by treatment with a moderate affinity Fe chelator like CQ. Similar experiments conducted with therapeutics with a higher affinity for Fe, such as deferiprone, which has shown great promise in reducing brain Fe load in PD,²² may provide more insight into whether neonatal Fe exposure, combined with the A53T mutation to α -syn is indeed a viable interventionist approach, considering our hypothesis that high dietary exposure during development may increase risk of neurodegeneration.¹¹

Finally, to assess the effects of neonatal Fe administration and CQ treatment on a parkinsonian motor phenotype, we examined locomotor activity at 5 months of age (as distance covered and time spent in movement in the open field test; [Supporting Information Table S2](#)), as described by Fredriksson et al.¹⁴ Neonatal Fe loading had a clear effect on locomotor activity, with Fe-fed WT animal showing a significant reduction in distance traveled within 20 min of the activity task compared to controls ($p < 0.05$). Iron-loaded adult WT mice covered a shorter distance during the habituation period (0–20 min block minus 40–60 min; $p < 0.05$; [Figure 4](#)), which was recovered by

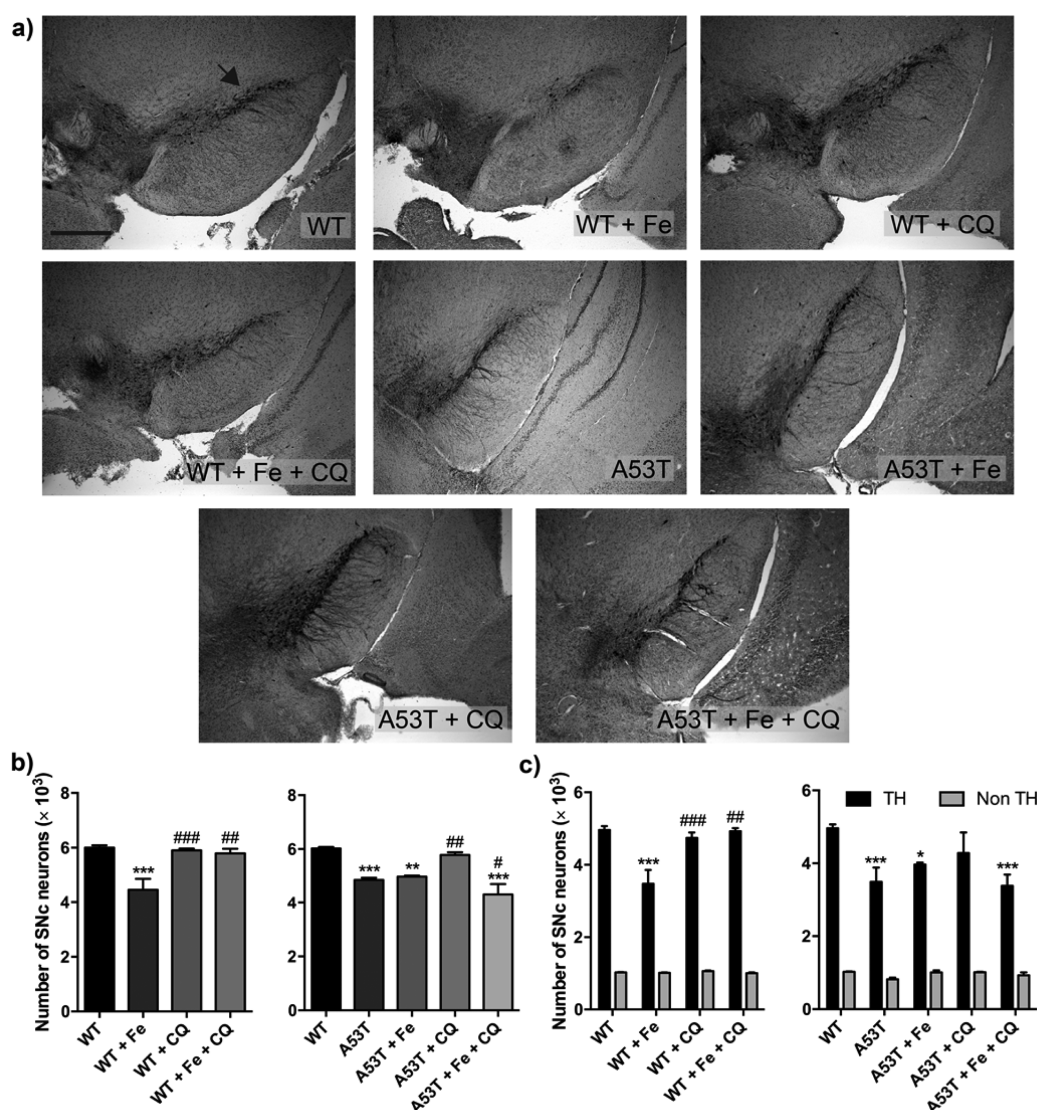


Figure 2. (a) Photomicrographs of TH positive neurons (stained black) at the level of the SNc (marked with a black arrow) in WT, A53T and treatment groups. Scale bar = 500 μ m. (b) Clioquinol treatment restored neuron numbers in the WT, Fe-loaded mice, and A53T mice without neonatal Fe exposure, though was unable to increase cell counts in the A53T + Fe treated animals (one-way ANOVA with Fisher's LSD test). (c) This effect was confined to dopaminergic (TH positive) neurons (* or # $p < 0.05$; ** or ### $p < 0.01$; *** or #### $p < 0.001$ one-way ANOVA with Fisher's LSD test; *compared to WT control; #compared to WT or A53T Fe supplementation).

CQ administration ($p < 0.05$), indicating early life Fe exposure impacted upon the animals' ability to ambulate specifically during exploration of a novel environment later in life. Habituation measurement assesses nonassociative learning by repetitive measurement of locomotive behavior.¹⁴ A reduction in habituation behavior is indicative of a deficiency in sensory, motor, cognitive and affective subsystems,²³ all of which involve the activity of dopamine. Clioquinol treatment had a significant effect on the distance traveled by A53T transgenic mice during the first two 20 min blocks (0–20 min = +33.0%; 20–40 min = +34.5%; $p < 0.05$), though no effect on habituation was observed in the A53T mice. Sustained motor activity in the 40–60 min block was dramatically reduced in the Fe-supplemented A53T mice compared to WT (−51.3%; $p < 0.01$). Regarding time spent in movement, Fe-fed WT mice showed bradykinesia during the first 20 min time block (−15.7%; $p < 0.01$), with a decreased propensity to explore novel environments or to habituate (−35.5%; $p < 0.05$). Clioquinol treatment restored normal time spent in movement in WT animals, and

demonstrated a similar effect on A53T mice versus Fe-fed transgenics during the 20–40 min block. In this group, sustained improvement in movement was not carried forward into the following 20 min periods, suggesting that CQ may modulate dopamine levels in an acute, time dependent manner. Iron-fed A53T mice became hypokinetic during the 40–60 min period (−48.7%; $p < 0.01$), suggesting that Fe in combination with the mutated α -syn protein prevents sustained motor activity; a feature not observed in the nonsupplemented transgenic animals.

These data further support PD being a multifaceted disorder, where a number of biochemical factors work in concert to produce a toxic cellular environment, and highlight a major limitation in animal models that do not represent a more comprehensive range of disease pathologies. Our results also suggest that loading of Fe into the brain during critical development windows represents an increased risk of parkinsonism when combined with elevated levels of human A53T mutation of α -syn; a risk that cannot be mitigated

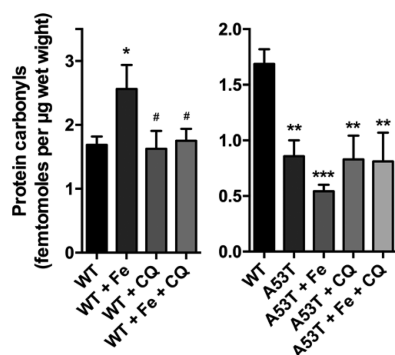


Figure 3. Protein carbonyls were significantly elevated in the Fe-loaded wild type mice, and these returned to control levels after CQ treatment. All A53T mice showed lower levels of protein carbonyls compared to WT, which may be an effect of the genotype, and there was no significant difference in protein carbonyl levels compared to Fe-loaded A53T mice, though this may be due to the small sample size used for the protein carbonyl assay ($n = 5$; * or # $p < 0.05$; ** $p < 0.01$; *** $p < 0.001$ one-way ANOVA with Fisher's LSD test; * compared to WT control; # compared to WT or A53T Fe supplementation).

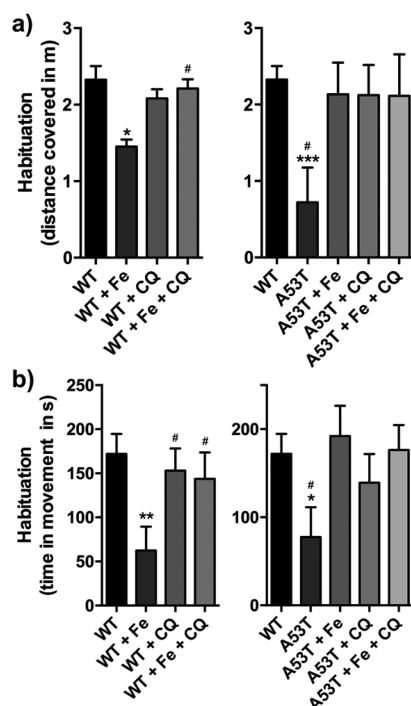


Figure 4. Habituation measured by the difference in both distance covered (a) and time spent in movement (b) was significantly decreased in Fe-loaded WT mice, with CQ treatment showing an improvement in habituation as measured by time in movement and distance covered for WT, Fe-loaded mice. Both measures showed a significant decrease in A53T mice compared to control (* or # $p < 0.05$; ** $p < 0.01$; one-way ANOVA with Fisher's LSD test; * compared to WT control; # compared to WT or A53T Fe supplementation.)

through Fe-chelation alone by a moderate affinity Fe-binding molecule. Clioquinol administration to Fe-loaded A53T mice reduced nigral Fe levels measured postmortem, but results from stereology and locomotor activity would suggest that Fe-mediated damage was irreversible when compared to the A53T mutation alone. While the A53T transgenic mouse does not exhibit cellular damage until later in life, these data suggest that,

at the molecular level, interactions between α -syn and Fe precipitate a toxicity that is irreparable by CQ. The A53T mutation has a higher propensity for α -syn to aggregate,²⁴ and our results suggest that high nigral Fe levels during early life may promote the formation of toxic oligomers earlier than observed in the non-Fe loaded A53T mouse. Further, these data suggest that the consequences of a Fe rich neuronal environment established in early life are important when the animal matures.

In PC12 cells and cultured rat primary midbrain neurons, overexpression of nonmutated α -syn results in Fe accumulation,²⁵ which may be exacerbated in nigral cells by excessive brain Fe. Additionally, lipopolysaccharide-induced nigrostriatal neurotoxicity has been shown to increase gut permeability, concomitant with increased α -syn expression in intestinal dopaminergic neurons.²⁶ In this case, overexpression of toxic A53T α -syn may be responsible for a similar effect, increasing the uptake of dietary Fe that ultimately crosses the developing blood-brain barrier.²⁷ Detailed investigation of the effects of α -syn overexpression in the gut on brain Fe metabolism warrants further study.

Clioquinol has spawned a range of analogues that are designed to improve blood-brain barrier permeability with reduced side effects,²⁸ and remains one of the original "ionophoric" compounds that initiated intensive research into metal ion modulation as a viable therapeutic strategy to address metal-mediated oxidative stress. However, mounting evidence that interactions between Fe and the α -syn protein may be a key upstream feature of PD²⁹ further supports the need to determine the mechanism of such compounds in animal models that recapitulate more than one molecular feature of the disease, which will in turn lead to better avenues of drug discovery.

CONCLUSIONS

Our results suggest that elevated Fe intake in the neonate specifically increases nigral metal levels in the adult, though it does not appear to further potentiate the already neurotoxic effects of the human A53T mutation of α -syn in mice. When treated with CQ, the observed recovery in both dopaminergic cells and locomotor activity in Fe-loaded WT mice and non-Fe loaded A53T mice were not recapitulated in the Fe-treated transgenic group. Considering the known associations between Fe and α -syn aggregation,⁵ it is plausible that increased nigral Fe arising from high neonatal exposure initiates aggregation earlier in this model. This work further confirms that CQ has an effect on mitigating the parkinsonian phenotype of the A53T mutation, though when combined with high nigral Fe levels the rescue of the disease features were not observed. We hypothesize that a Fe chelator with a higher affinity for Fe may provide beneficial effects in the combined Fe-loading and A53T model, and are now continuing this line of enquiry.

METHODS

Animals. All procedures involving transgenic mice and wild type (WT) C57BL/6 mice conformed to the Australian National Health and Medical Research Council Code of Practice and were approved by the University of Melbourne ethics committee. All experiments were designed to minimize the number of animals used, pain, and discomfort, while still providing statistically significant populations. Pregnant C57BL/6 and $^{+/+}$ (h)A53T mice were housed in separate cages at 22 °C with a 12 h light/dark cycle. The mothers had access to normal rodent chow and water ad libitum at all times.

Iron Treatment. All mice pups were fed either 8% sucrose in water vehicle or vehicle plus iron by oral gavage between days 10 and 17 postpartum. These pups were later divided into four treatment groups (vehicle; +Fe; +CQ; +Fe+CQ). Iron supplementation was a carbonyl iron (Sigma-Aldrich; catalog no. C3518), following the protocol reported by Kaur et al.¹² shown to increase nigral iron levels in later life. Carbonyl Fe has been reported to be more bioavailable than ferrous (Fe^{2+}) salts with a lesser side effect profile.³⁰ Pups were weighed and administered iron at 0.12 mg kg^{-1} body weight. Body weight was recorded daily.

Clioquinol Administration. Animals commenced CQ feeding from 12 weeks of age. Mice were fed a diet of standard rodent chow (Glenforrest Stockfeeders, Australia) supplemented with 250 mg kg^{-1} CQ (Sigma-Aldrich, Australia). It was determined that a 12 week old mouse consumed 4 g of CQ containing food daily, corresponding to an average daily dose of 37 mg kg^{-1} CQ per day. Animals received this diet for approximately 5 months before culling.

Locomotor Activity. Spontaneous motor activity was measured using a photobeam activity system (Truscan 2.0, Coulbourn Instruments) as described by Fredriksson et al.¹⁴ A cage 25.4 cm wide, 25.4 cm deep, and 40.6 cm high was used, with beams evenly spaced at 1.5 cm intervals. Parameters of movement were calculated from the mouse's interception of the beams to provide an xy coordinate. Total distance moved (sum of all vectored coordinate changes in cm) and total time spent in motion (sum of elapsed time for all movements in seconds) was measured. Movement data was recorded in 5 min bins, which were pooled into 20 min blocks. The 0–20 min block was defined as “exploratory activity”, and a value for “habituation” was calculated by subtracting the values obtained during the 0–20 min period from the 40–60 min block. Tests were conducted on animals at 5 months of age.

Tissue Collection. At 8 months of age, animals were anesthetized using sodium pentobarbitone (100 mg kg^{-1} ; Lethobarb; Virbac, Australia). Once involuntary reflexes were absent, the animals were transcardially perfused using 25 mL of cold phosphate buffered saline ($\text{pH } 7.4$; 0.1 M) containing 0.5% butylated hydroxytoluene (Sigma-Aldrich) to protect protein carbonyl species from oxidative damage during the procedure. The brain was then removed from the skull and frozen on dry ice and stored at -80°C until use. Brains were used for either biochemical analysis or immunohistochemistry.

Tissue was collected from cortex (CTX), cerebellum (CB), caudate putamen (CPU), and substantia nigra pars compacta (SNc) using a chilled, chrome-coated steel mouse brain matrix (Plastics One Inc.). The brain was aligned with the ventral side exposed, and the optic chiasm used the key landmark for consistent dissection. Samples were stored in metal-free 1.5 mL polypropylene tubes (Techno Plas, Australia) prior to analysis.

Iron Analysis. Samples were weighed and then lyophilized overnight, before $100\text{--}300 \mu\text{L}$ (depending on sample size) of 65% Suprapur grade nitric acid (BDH, U.K.) was added to the 1.5 mL tube. Samples were heated to 90°C for 20 min, and then an equal volume of 30% hydrogen peroxide (BDH) was added to aid digestion of lipids. Samples were then heated to 70°C for an additional 15 min before a $40 \mu\text{L}$ aliquot of the reduced digest volume was made to 1.0 mL with 1% nitric acid. Lyophilized bovine liver (1577b; NIST) was used for quality control purposes. Metal analysis was performed on a Varian UltraMass 700 spectrometer (Varian, Australia) using routine conditions. A $100 \mu\text{g L}^{-1}$ solution of yttrium was introduced via a T-piece, with $m/z = 89$ used as the internal standard mass. All concentrations are reported as $\mu\text{g g}^{-1}$ wet weight of the original tissue sample.

Histological Determination of Cell Numbers. For immunohistochemical analysis and stereological estimates of SNc neuron numbers, brains were removed from the skull and immediately placed in 15 mL of 4% paraformaldehyde (PFA) in phosphate buffered saline (PBS; $\text{pH } 7.4$; 0.2 M) at 4°C overnight, followed by two daily changes of 30% sucrose in PBS. Brains were sectioned at $30 \mu\text{m}$ thickness in a series of 3 in the coronal plane from the anterior end of the SNc. Sections were placed on gelatin-coated microscope slides and dried at

room temperature for 20–30 min, and then stored at -80°C prior to histological staining.

One series from each brain was used for TH immunohistochemistry to identify dopaminergic neurons in the SNc. Sections were briefly fixed in 4% PFA for 30 s, and then rinsed in three changes of Tris-buffered saline and Tween 20 (TBST; $\text{pH } 8.0$). Sections were blocked in 3% normal goat serum (NGS; Merk Millipore) for 15 min at room temperature, and then rinsed again three times in TBST. Sections were incubated overnight at room temperature with a primary polyclonal anti-rabbit TH antibody (Merk Millipore), diluted 1 in 3000. After incubation, samples were again rinsed in TBST and incubated for 1 h at room temperature with a secondary horseradish peroxidase (HRP) conjugated polyclonal goat anti-rabbit HRP antibody (Merk Millipore). Staining was visualized using diaminobenzidine (DAB) enhancement with cobalt and nickel. Sections were counterstained with neutral red, dehydrated, cleared, and mounted with a coverslip.

Neurons were estimated using a stereological fractionator design as previously described.^{31,32} The SNc was delimited a $10\times$ magnification, and neurons distinguished according to their size ($16 \mu\text{m}$ soma) compared to the adjacent smaller ($13 \mu\text{m}$ soma) dopaminergic neurons in the rostral ventral tegmental area. Neurons were counted according to optical fractionator rules,^{33,34} and TH positive and negative neurons were scored within the SNc. A selection of a series of random sampled sections were taken at a random starting point, and neurons counted within an unbiased counting frame ($x = 35 \mu\text{m}$; $y = 45 \mu\text{m}$; $1575 \mu\text{m}^2$ total area) at regular intervals on a sampling grid of $140 \times 140 \mu\text{m}^2$. Counts were estimated using StereoInvestigator (MicroBrightfield) and viewed with a $60\times$ 1.3 NA oil objective lens (Leica, Australia). The total population of estimated cells was determined as the product of the total counted cells, $1/\text{ssf}$ and $1/\text{asf}$, where ssf is the section-sampling fraction (i.e., 1 of each 3 sections) and asf is the area of sampling fraction. Coefficients of error were calculated to determine which cell population estimates were significant.

Detection of Protein Carbonyls. Protein carbonyls are products and biomarkers of oxidative stress. The production of protein carbonyls involves oxidative reactions with ozone or oxides of nitrogen or by metal, in this case Fe, catalyzed oxidation. The modification of proteins by the addition of carbonyl groups occurs in the protein side chain. The carbonyls within the side chain can undergo derivatization to dinitrophenylhydrazones (DNP-hydrazone) when reacting with 2,4-dinitrophenylhydrazine (DNPH). The DNP-hydrazone moiety can be detected using a primary antibody. The carbonyls were detected with a kit (OxyBlot™ Protein Oxidation Detection Kit, Millipore) that provided the chemical and immunological reagents necessary to perform the quantitative immunoblot detection of carbonyl groups.

Tissues were weighed and homogenized in a 1.5 mL microfuge tube (Pathtec, Australia). The homogenization buffer contained 50 mL of Dulbecco's PBS (Cu and Mg-free; Sigma-Aldrich) and 1 tablet of Complete EDTA-free protease inhibitor (Roche, Australia) to prevent further protein degradation. This buffer was left to dissolve in a cold room at 4°C on a rocker. Then 0.5 M butylated hydroxytoluene (BHT; 2,6-bis(1,1-dimethylethyl)-4-methylphenol; Sigma-Aldrich) was dissolved in 1 mL of acetonitrile (Scharlau, Barcelona). The ratio of tissue to buffer was 1:5 (0.2 g tissue in 1 mL of buffer). PBS (containing protease inhibitor) was added to each sample while on ice. Following this, BHT was added to each sample to prevent further oxidation reactions from occurring. Brain samples were homogenized (while on ice) using a sonicator blade (Branson Sonifier 450, $1/8''$ microtip taper blade, Australia) for one to two pulses and one 30 s rest period. To obtain a homogeneous total lysate, the sample was centrifuged at $10\,000g$ for 5 min at 4°C . The supernatant was removed and the pellet fraction was kept at -80°C . A BCA assay was performed on the supernatant fraction to determine the protein content of the sample (Pierce). Only the supernatant fraction was further analyzed.

The samples were aliquoted into clean microcentrifuge tubes, each at a standard concentration of $10 \mu\text{g } \mu\text{L}^{-1}$ of protein, and then diluted to $5 \mu\text{L}$ with MilliQ H_2O . Duplicate aliquots were prepared for each sample: one for the DNPH reaction and the other for the control

reaction. The samples were denatured using 12% sodium dodecyl sulfate (SDS) to give a final SDS concentration of 6%. The derivatization of the samples was performed by adding 10 μ L of the 1 \times DNPH solution to one of the duplicates and 10 μ L of the 1 \times control DNPH solution to the other. These reactions were left to incubate for 15 min at room temperature and were neutralized using 7.5 μ L of the neutralizing solution. The samples were then blotted directly onto a nitrocellulose membrane (BioRad) using a dot blot apparatus. One hundred femtomoles of internal standard (OxyBlot Protein standard, Millipore) was run with the samples.

The membrane was left to block in 1% BSA/PBST for 1 h on a rocker. After the 1 h incubation, the membrane was incubated with the primary antibody (rabbit anti-DNP, Millipore), diluted at 1:150 in 1% BSA/PBST for 1 h using gentle rocking at room temperature. The membrane was rinsed twice with PBST, before a 15 min PBST wash. The secondary antibody (goat anti-rabbit IgG HRP conjugated, Millipore) was diluted to 1:300 in 1% BSA/PBST and incubated with the membrane for 1 h at RT with gentle rocking. The membrane was rinsed twice and washed with PBST. The chemiluminescent reagents (Amersham ECL, GE Healthcare, Sweden) were prepared using equal volumes. The membrane was covered with the solution and incubated for 1 min prior to exposure. The luminescent membrane was placed onto a Fuji imaging system (Japan) to detect the fluorescence signal.

With the use of the internal standard, the derivatized samples were quantified using a multigauge imaging system (Fujifilm Corporation, Japan). Determination of oxidative modification was performed by comparing all samples to the internal control. The internal standard was composed of five proteins that contain one to three DNP residues. Analyzed spectrophotometrically, 2.5 μ L of the internal standard correlated to 100 fmol of DNP residues. The optical density of each sample was determined by extrapolating from the results of the internal standard, and expressed as a percentage ratio (of 100 fmol) minus PBS (pH 7.4) background. Each sample was then adjusted for weight and expressed as femtomoles per wet weight of tissue.

Statistical Analysis. Statistical analysis was performed using Prism 6 (GraphPad), using a one-way ANOVA followed by a complementary Fisher's least-squares difference (LSD) post hoc test. This test was chosen to compare control and Fe-supplemented groups independently.

■ ASSOCIATED CONTENT

■ Supporting Information

The Supporting Information is available free of charge on the ACS Publications website at DOI: 10.1021/acscchemneuro.5b00305.

Regional brain Fe concentrations (Table S1) and locomotor activity testing data (Table S2) (PDF)

■ AUTHOR INFORMATION

Corresponding Author

*E-mail: david.finkelstein@florey.edu.au.

Author Contributions

[§]J.L.B. and D.J.H. contributed equally. J.L.B., D.J.H., R.A.C., A.I.B., P.A.A., and A.I.B. conceived and designed the study. J.L.B., M.N., and I.V. performed the experiments. J.L.B., D.J.H., and D.I.F. analyzed the data and wrote the manuscript. All authors edited and approved the final version of the manuscript.

Funding

D.J.H., P.A.A., R.A.C., A.I.B., and D.I.F. are supported by funds from the National Health and Medical Research Council and the Australian Research Council. The Florey Institute of Neuroscience and Mental Health acknowledge the strong support from the Victorian Government and in particular the funding from the Operational Infrastructure Support Grant.

Notes

The authors declare the following competing financial interest(s): R.A.C., P.A.A., and D.I.F. are shareholders and scientific consultants to Prana Biotechnology Ltd. A.I.B. is a shareholder in Mesoblast Ltd, Cogstate Ltd, Brighton LLC, Prana Biotechnology Ltd, Eucalyptus LLC, and is a paid consultant for Collaborative Medicinal Discovery LLC and Brighton LLC.

■ REFERENCES

- (1) Hare, D. J., Ayton, S., Bush, A., and Lei, P. (2013) A delicate balance: Iron metabolism and diseases of the brain. *Front. Aging Neurosci.* 5, 34.
- (2) Ward, R. R., Zucca, F. A., Duyn, J. H., Crichton, R. R., and Zecca, L. (2014) The role of iron in brain ageing and neurodegenerative disorders. *Lancet Neurol.* 13, 1045–1060.
- (3) Zecca, L., Stroppolo, A., Gatti, A., Tampellini, D., Toscani, M., Gallorini, M., Giaveri, G., Arosio, P., Santambrogio, P., Fariello, R. G., et al. (2004) The role of iron and copper molecules in the neuronal vulnerability of locus coeruleus and substantia nigra during aging. *Proc. Natl. Acad. Sci. U. S. A.* 101, 9843.
- (4) Li, J., Uversky, V. N., and Fink, A. L. (2001) Effect of Familial Parkinson's Disease Point Mutations A30P and A53T on the Structural Properties, Aggregation, and Fibrillation of Human α -Synuclein. *Biochemistry* 40, 11604–11613.
- (5) Ostrerova-Golts, N., Petrucelli, L., Hardy, J., Lee, J. M., Farer, M., and Wolozin, B. (2000) The A53T alpha-synuclein mutation increases iron-dependent aggregation and toxicity. *J. Neurosci.* 20, 6048–6054.
- (6) Hare, D. J., Lei, P., Ayton, S., Roberts, B. R., Grimm, R., George, J. L., Bishop, D. P., Beavis, A. D., Donovan, S. J., McColl, G., Volitakis, I., Masters, C. L., Adlard, P. A., Cherny, R. A., Bush, A. I., Finkelstein, D. I., and Doble, P. A. (2014) An iron–dopamine index predicts risk of parkinsonian neurodegeneration in the substantia nigra pars compacta. *Chem. Sci.* 5, 2160–2169.
- (7) Finkelstein, D. I., Hare, D. J., Billings, J. L., Sedjahtera, A., Nurjono, M., Arthofer, E., George, S., Culvenor, J. G., Bush, A. I., and Adlard, P. A. (2015) Clioquinol Improves Cognitive, Motor Function, and Microanatomy of the Alpha-Synuclein hA53T Transgenic Mice. *ACS Chem. Neurosci.*, DOI: 10.1021/acscchemneuro.5b00253.
- (8) Bareggi, S. R., and Cornelli, U. (2012) Clioquinol: review of its mechanisms of action and clinical uses in neurodegenerative disorders. *CNS Neurosci. Ther.* 18, 41–46.
- (9) Kaur, D., Yantiri, F., Rajagopalan, S., Kumar, J., Mo, J. Q., Boonplueang, R., Viswanath, V., Jacobs, R., Yang, L., Beal, M. F., DiMonte, D., Volitakis, I., Ellerby, L., Cherny, R. A., Bush, A. I., and Andersen, J. K. (2003) Genetic or pharmacological iron chelation prevents MPTP-induced neurotoxicity in vivo: a novel therapy for Parkinson's disease. *Neuron* 37, 899–909.
- (10) Hare, D. J., Adlard, P. A., Doble, P. A., and Finkelstein, D. I. (2013) Metallobiology of 1-methyl-4-phenyl-1,2,3,6-tetrahydropyridine neurotoxicity. *Metallomics* 5, 91–109.
- (11) Hare, D. J., Arora, M., Jenkins, N. L., Finkelstein, D. I., Doble, P. A., and Bush, A. I. (2015) Is early-life iron exposure critical in neurodegeneration? *Nat. Rev. Neurol.* 11, 536–544.
- (12) Kaur, D., Rajagopalan, S., Cherny, R. A., and Andersen, J. K. (2007) Increased murine neonatal iron intake results in Parkinson-like neurodegeneration with age. *Neurobiol. Aging* 28, 907–913.
- (13) Fredriksson, A., Schröder, N., Eriksson, P., Izquierdo, I., and Archer, T. (1999) Neonatal Iron Exposure Induces Neurobehavioural Dysfunctions in Adult Mice. *Toxicol. Appl. Pharmacol.* 159, 25–30.
- (14) Fredriksson, A., Schröder, N., Eriksson, P., Izquierdo, I., and Archer, T. (2001) Neonatal iron potentiates adult MPTP-induced neurodegenerative and functional deficits. *Parkinsonism Relat. Disord.* 7, 97–105.
- (15) Ayton, S., and Lei, P. (2014) Nigral Iron Elevation Is an Invariable Feature of Parkinson's Disease and Is a Sufficient Cause of Neurodegeneration. *BioMed Res. Int.* 2014, 1–9.

- (16) Giasson, B. I.; Duda, J. E.; Quinn, S. M.; Zhang, B.; Trojanowski, J. Q.; and Lee, V. M. Y. (2002) Neuronal α -Synucleinopathy with Severe Movement Disorder in Mice Expressing A53T Human α -Synuclein. *Neuron* 34, 521–533.
- (17) Hare, D. J.; Lee, J. K.; Beavis, A. D.; van Gramberg, A.; George, J.; Adlard, P. A.; Finkelstein, D. I.; and Doble, P. A. (2012) Three-dimensional atlas of iron, copper, and zinc in the mouse cerebrum and brainstem. *Anal. Chem.* 84, 3990–3997.
- (18) Bacopoulos, N. G., and Bhatnagar, R. K. (1977) Correlation between tyrosine hydroxylase activity and catecholamine concentration or turnover in brain regions. *J. Neurochem.* 29, 639–643.
- (19) Oaks, A. W.; Frankfurt, M.; Finkelstein, D. I.; and Sidhu, A. (2013) Age-Dependent Effects of A53T Alpha-Synuclein on Behavior and Dopaminergic Function. *PLoS One* 8, e60378.
- (20) Hung, L. W.; Villemagne, V. L.; Cheng, L.; Sherratt, N. A.; Ayton, S.; White, A. R.; Crouch, P. J.; Lim, S.; Leong, S. L.; and Wilkins, S. (2012) The hypoxia imaging agent CuII (atasm) is neuroprotective and improves motor and cognitive functions in multiple animal models of Parkinson's disease. *J. Exp. Med.* 209, 837–854.
- (21) Ryan, T. M.; Roberts, B. R.; McColl, G.; Hare, D. J.; Doble, P. A.; Li, Q.-X.; Lind, M.; Roberts, A. M.; Mertens, H. D. T.; Kirby, N.; Pham, C. L. L.; Hinds, M. G.; Adlard, P. A.; Barnham, K. J.; Curtain, C. C.; and Masters, C. L. (2015) Stabilization of nontoxic A β -oligomers: insights into the mechanism of action of hydroxyquinolines in Alzheimer's disease. *J. Neurosci.* 35, 2871–2884.
- (22) Devos, D.; Moreau, C.; Devedjian, J. C.; Kluza, J.; Petrault, M.; Laloux, C.; Jonneaux, A.; Ryckewaert, G.; Garçon, G.; Rouaix, N.; Duhamel, A.; Jissendi, P.; Dujardin, K.; Auger, F.; Ravasi, L.; Hopes, L.; Grolez, G.; Firdaus, W.; Sablonnière, B.; Strubi-Vuillaume, I.; Zahr, N.; Destée, A.; Corvol, J.-C.; Pörtl, D.; Leist, M.; Rose, C.; Defebvre, L.; Marchetti, P.; Cabantchik, Z. I.; and Bordet, R. (2014) Targeting chelatable iron as a therapeutic modality in Parkinson's disease. *Antioxid. Redox Signaling* 21, 195–210.
- (23) Fredriksson, A.; Schröder, N.; Eriksson, P.; Izquierdo, I.; and Archer, T. (2000) Maze learning and motor activity deficits in adult mice induced by iron exposure during a critical postnatal period. *Dev. Brain Res.* 119, 65–74.
- (24) Olivares, D.; Huang, X.; Branden, L.; Greig, N.; and Rogers, J. (2009) Physiological and Pathological Role of Alpha-synuclein in Parkinson's Disease Through Iron Mediated Oxidative Stress; The Role of a Putative Iron-responsive Element. *Int. J. Mol. Sci.* 10, 1226–1260.
- (25) Ortega, R.; Carmona, A.; Roudeau, S.; Perrin, L.; Dučić, T.; Carboni, E.; Bohic, S.; Cloetens, P.; and Lingor, P. (2015) α -Synuclein Over-Expression Induces Increased Iron Accumulation and Redistribution in Iron-Exposed Neurons. *Mol. Neurobiol.* DOI: 10.1007/s12035-015-9146-x.
- (26) Kelly, L. P.; Carvey, P. M.; Keshavarzian, A.; Shannon, K. M.; Shaikh, M.; Bakay, R. A. E.; and Kordower, J. H. (2014) Progression of intestinal permeability changes and alpha-synuclein expression in a mouse model of Parkinson's disease. *Mov. Disord.* 29, 999–1009.
- (27) Taylor, E. M.; Crowe, A.; and Morgan, E. H. (1991) Transferrin and Iron Uptake by the Brain: Effects of Altered Iron Status. *J. Neurochem.* 57, 1584–1592.
- (28) Barnham, K. J., and Bush, A. I. (2014) Biological metals and metal-targeting compounds in major neurodegenerative diseases. *Chem. Soc. Rev.* 43, 6727–6749.
- (29) Deas, E.; Cremades, N.; Angelova, P. R.; Ludtmann, M.; Yao, Z.; Chen, S.; Horrocks, M.; Banushi, B.; Little, D.; Devine, M.; Gissen, P.; Klenerman, D.; Dobson, C.; Wood, N.; Gandhi, S.; and Abramov, A. Y. (2015) Alpha-synuclein oligomers interact with metal ions to induce oxidative stress and neuronal death in Parkinson's disease. *Antioxid. Redox Signaling*. DOI: 10.1089/ars.2015.6343.
- (30) Sacks, P. V., and Houchin, D. N. (1978) Comparative bioavailability of elemental iron powders for repair of iron deficiency anemia in rats. Studies of efficacy and toxicity of carbonyl iron. *Am. J. Clin. Nutr.* 31, 566–571.
- (31) Finkelstein, D. I.; Stanic, D.; Parish, C. L.; Tomas, D.; Dickson, K.; and Horne, M. K. (2000) Axonal sprouting following lesions of the rat substantia nigra. *Neuroscience* 97, 99–112.
- (32) Ayton, S.; Lei, P.; Duce, J. A.; Wong, B. X. W.; Sedjahtera, A.; Adlard, P. A.; Bush, A. I.; and Finkelstein, D. I. (2013) Ceruloplasmin dysfunction and therapeutic potential for Parkinson disease. *Ann. Neurol.* 73, 554–559.
- (33) Gundersen, H. J.; Bagger, P.; Bendtsen, T. F.; Evans, S. M.; Korbo, L.; Marcussen, N.; Møller, A.; Nielsen, K.; Nyengaard, J. R.; Pakkenberg, B.; Sørensen, F. B.; Vesterby, A.; and West, M. J. (1988) The new stereological tools: disector, fractionator, nucleator and point sampled intercepts and their use in pathological research and diagnosis. *APMIS* 96, 857–881.
- (34) Parish, C. L.; Stanic, D.; Drago, J.; Borrelli, E.; Finkelstein, D. I.; and Horne, M. K. (2002) Effects of long-term treatment with dopamine receptor agonists and antagonists on terminal arbor size. *Eur. J. Neurosci.* 16, 787–794.